Research Article Vol. 11, No. 3 / 1 March 2021 / Optical Materials Express 757
Optical Materials EXPRESS

Spectroscopy of GR1 centers in synthetic diamonds

SHOVA SUBEDI,[1,*] VLADIMIR FEDOROV,[1] SERGEY MIROV,[1] AND MATTHEW MARKHAM[2]

[1]The Department of Physics, University of Alabama at Birmingham, CH 310, 1300 University Blvd., Birmingham, AL 35294, USA
[2]Element Six (UK) Limited, Global Innovation Centre, Harwell Campus, Oxfordshire, OX110QR, UK
[*]shova1@uab.edu

Abstract: We report on the spectroscopic characterization, absorption saturation, and excited-state dynamics of GR1 centers in synthetic diamonds. The non-linear optical measurements reveal an efficient bleaching of the GR1 center's ground level under ns-pulsed 633 nm excitation. The maxima of absorption and emission cross sections were estimated to be 4.5×10^{-17} cm^2 and 9×10^{-17} cm^2 at 630 nm and 780 nm, respectively. The radiative lifetime of the excited level was estimated to be 8.5 ns. The 658 nm probe kinetics uncovered relaxation of $^1T_2$ excited level going predominantly to a metastable state with a lifetime of 220 µs. An induced absorption detected with the use of a highly concentrated diamond sample could be due to up-conversion and photoionization processes in additional impurity-vacancy center with absorption at the short-wavelength tail of GR1. The results presented here indicate that synthetic diamonds with GR1 centers could serve as near infrared gain media or passive Q-switchers for laser cavities over the 633–750 nm spectral range. Optimization of the center concentration and the crystal parameters are required to minimize the induced absorption at the lasing wavelengths.

1. Introduction

Color center diamond crystals are unique media with great potential for a wide range of photonics applications due to their thermal and photochemical stability as well as interesting optical properties [1]. The GR1 center in diamonds is a common optical center created by ionizing radiation exposure and attributed to the neutral monovacancy of the carbon atom (V^0) [2–4]. These centers are strongly luminescent at and above room temperature and are thermally stable at temperatures of several hundred of degrees Celsius [5,6]. The center has a tetrahedral (T_d) point symmetry [7]. The orbitally degenerated energy level splits-up due to Jahn-Teller interactions [8,9]. The ground state splits into two sublevels, namely ^1E and $^1A_1$, separated by 8 meV [10,11]. The transition from the lowest ground level ^1E to the first excited state $^1T_2$ features a sharp zero phonon line (ZPL) at 1.673 eV (741 nm) with a phonon assisted absorption band within the red spectral region [3,10,12]. The origin of the weak ZPL at 1.665 eV (744 nm) is attributed to the thermally populated $^1A_1$ state from the ^1E level [7,12–14]. The additional lines, designated by GR2 to GR8, are observed in the absorption spectrum between 411 nm and 430 nm due to transitions to higher excited states [15]. However, no photoluminescence (PL) was identified for transitions from the high lying excited states directly to the ground state [15]. Also, the direct (632.8 nm) and indirect excitations (410 nm to 435 nm) via GR1 and GR2-GR8 absorption bands resulted in the same PL corresponding to the GR1 emission [16]. Under GR2-GR8 excitation, the GR1 center relaxes non-radiatively to the first excited state followed by a characteristic GR1 PL [16,17]. The PL lifetime was reported to be 2.5 ns and 1.1 ns at 70 K and 300 K, respectively. The estimated radiative lifetime was 182 ns at 70 K which implies non- radiative transition as a dominant relaxation channel [18]. Previously reported time-resolved spectroscopy

#417432 https://doi.org/10.1364/OME.417432
Journal © 2021 Received 11 Dec 2020; revised 29 Jan 2021; accepted 30 Jan 2021; published 12 Feb 2021

Optical Materials EXPRESS

under nanosecond excitation of the GR1 center showed nearly uniform decay constant with no susceptible quenching as featured by other nitrogen and vacancy related centers [3,19].

Laser action of H3 centers (a vacancy adjacent to two substitutional nitrogen atoms) in natural [6] and synthetic diamonds [21] have already been documented more than two decades ago. Unfortunately, no notable progress has been reported on the lasing application of color centers in diamonds until recently [20]. With the advancement in commercial fabrication technology and improved understanding of the properties of the color center, these media are promising for practical laser applications [21]. The saturation of absorption of GR1 centers under Ruby laser radiation was reported in [22]. It indicates the possibility of the utilization of GR1 centers for many laser applications. However, for applications such as gain media and passive Q-switching of laser cavities, it is very crucial to fully understand the relaxation process after excitation to $^1T_2$ level. The present research reports on the optical characterization, nonlinear absorption, and relaxation processes in crystals with different concentrations of GR1 centers. The feasibility of color center diamond crystals as an active gain media with frequency tunability in visible to near infrared region as well as Q-switching of laser cavities has been analyzed.

2. Experimental details

The samples used in this experiment were micro-plasma enhanced chemical vapor deposition (CVD) grown bulk diamonds from Element 6. Two diamond samples, designated as HD and LD, having different GR1 concentrations were utilized. The dimensions of the samples were $4\times3\times1$ mm^3. The diamond crystals had initial nitrogen concentration [N]~0.15 ppm and were essentially free from other impurities (type IIa). The samples were further irradiated using a 4.5 MeV electron source with a beam current of 20 mA and an estimated density of 2.5×10^{14} cm^{-2}s^{-1}. The HD and LD samples were electron irradiated for about 10 hours and 4 hours, respectively. The absence of other donor and acceptor impurities in the crystal ensures the vacancies are predominantly in the neutral charge state (V^0). The center imparts bluish-greenish coloration to the crystal. The transmission spectra were collected using a Shimadzu UV-Vis-NIR 3101-PC spectrophotometer at room temperature. The optical excitation and pump-probe experiments were carried out using 633 nm pump radiation (Deuterium Raman shifted radiation of a Q-switched 532 nm Nd:YAG laser operating at 10 Hz with a pulse duration of 4.5 ns). The PL signal was measured and detected using an Acton Research Corporation 750 spectrometer and R5108 photomultiplier tube from Hamamatsu and amplified using a gated boxcar integrator from Stanford Instruments. In the pump-probe experiments, CW radiation of 532 nm and 658 nm lasers with power ~15 mW were used as probe beams.

3. Results and discussions

3.1. Visible and NIR absorption and PL spectra

Room temperature transmission spectra of two samples corresponding to the $^1E\rightarrow{}^1T_2$ transition are depicted in Fig. 1(A). The spectra were collected with 1 nm spectral resolution at a slow scanning speed of 100 nm/min. The spectra show the GR1 characteristic ZPL absorption at 741 nm, along with the vibronic band extending from 500 nm to 780 nm. The CVD growth process was carried out in atomic hydrogen rich environment. The absorption lines near 900 nm and 1075 nm are similar to the sharp peaks observed in hydrogen-rich diamond and this feature is attributed to hydrogen-related centers [1,23]. As one can see from Fig. 1 (A), the GR1 absorption band overlaps with additional parasitic centers with a band peak near 350 nm. Previously, similar features were reported in absorption spectra and ascribed to negative interstitial vacancy (ND1) centers in type I diamonds. The energy transfer process between ND1 and GR1 centers was triggered under thermal and optical excitation [10,24]. The 350 nm UV band studied in [24] is very similar to what we observed in our absorption spectra. We believe that the absorption

Optical Materials EXPRESS

band near 350 nm is due to absorption of ND1 centers alone or other impurity centers originated due to irradiation may also present in addition to ND1 centers. To compare the relative strength of UV absorption bands in our samples, we normalized the LD absorption spectrum to the value of HD absorption at 630 nm, where GR1 absorption dominates. Figure 1(B) shows the absorption spectrum of the HD sample (red curve) as well as the absorption spectrum of the LD sample multiplied by factor 6.3 (blue dashed curve). The baseline is shown in green short-dashed curve in Fig. 1(B). To estimate the background, we use the 3rd order polynomial regression of absorption coefficient.

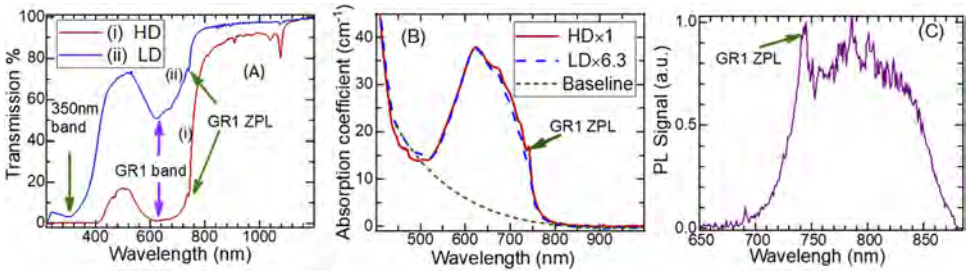

Fig. 1. (A) Transmission spectra of HD (curve i) and LD (curve ii) samples at room temperature; (B) GR1 absorption spectra of the HD (curve i) and LD (curve ii) samples normalized near 630 nm; (C) The normalized emission spectra measured under pulsed 633 nm excitation and calibrated with respect to the sensitivity of spectrometer-detector system.

Excitation with 633 nm radiation resulted in a luminescence band spanning over the 700 nm - 870 nm range with a sharp ZPL at 741 nm as shown in Fig. 1(C). The PL signal was strong and easily detectable even with the closed slits of the spectrometer. The graph in Fig. 1(C) was calibrated with respect to sensitivity of the spectrometer-detector combination using an Oriel standard calibration lamp (model# 63358) and normalized to 1. The pulse duration (~4.2 ns) is longer than the reported lifetime of $^1T_2$ deactivation (1.1 ns) at room temperature [18]. Hence, the excited state lifetime cannot be directly measured with the current pump pulse.

3.2. *Pump-probe experiment under nanosecond excitation*

In the present section, we studied the dynamics of absorption at possible oscillation wavelengths after excitation at room temperature. The pump-probe experiment was conducted using two CW probe beams at 658 nm and 532 nm and the measured kinetics were compared for both diamond samples. The experimental setup of the pump-probe measurement is shown in Fig. 2. In this case, the pump and probe beams were sent collinearly through the sample and the pump-induced change in transmission of the CW probe beam was measured. To analyze the dynamics of the saturation and excited state absorption at the probe beams, we plotted the normalized kinetics as $-(k_0 - k(t))/k_0 = -\Delta k/k_0$, where k_0 is the initial absorption coefficient and $k(t)$ represents its temporal evolution after pulse excitation at probe wavelength. In the case of a single excitation center without excited state absorption (ESA), this ratio does not depend on the absorption cross section and should be the same for both probe beams. The ratio $(\Delta k/k_0)$ is proportional to fractional population inversion $(\Delta N/N_0)$ and gives the kinetics of population inversion and recovery of the centers to the original energy level. In this notation, a positive value corresponds to the saturation of the sample absorption while a negative value indicates the presence of induced or excited state absorption.

Figures 3(A), 3(B), and 3(C) show temporal profiles of the 658 nm probe beam recorded at different timescales for HD (orange curves (i)) and LD (blue curves (ii)) samples. The temporal response time of the detection platform was longer than the excited level lifetime of GR1 centers.

Optical Materials EXPRESS

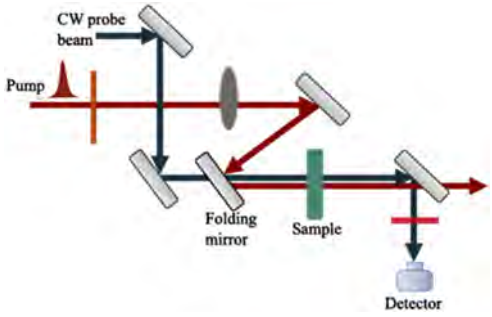

Fig. 2. Experimental setup of the pump-probe experiment.

As one can see from Fig. 3(A), we observed the absorption saturation at probe wavelength for both samples. In the case of the LD sample, the saturation spike is seen at the beginning of kinetics followed by a slow relaxation to the initial stage with a lifetime of 220 μs. The amplitude of the initial spikes is approximately the same as the amplitude of slow relaxation. It indicates that the relaxation from the $^1T_2$ state occurs predominantly via the metastable state.

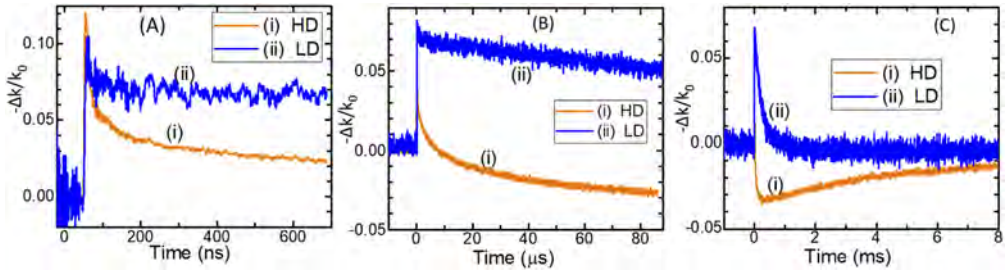

Fig. 3. The kinetics of 658 nm CW probe beam at (A) nanosecond, (B) microsecond, and (C) millisecond timescales for HD and LD samples shown in orange (curves (i)) and blue (curves (ii)), respectively.

The kinetics of the HD samples show a more complicated behavior. After initial saturation, we observed an induced absorption with a rise time of 44 μs [see Figs. 3(A) and 3(B)] followed by a non-exponential decay with a lifetime close to several milliseconds [see Fig. 3(C)]. The induced absorption was bigger than the ground state absorption that is why the curve (i) falls below zero. This indicates that the induced absorption cross section was larger than the absorption cross section of GR1 CCs at 658 nm. All the signals recover to the original level before another pulse. No long-term bleaching or residual absorption at a 10 Hz repetition rate were measured. The rise time of induced absorption differs from the lifetime of the $^1T_2$ state (1.1 ns) and the lifetime of the metastable state (220 μs), and, therefore, it could not be due to an energy transfer from the GR1 center to other CCs.

The kinetics of the 532 nm probe beam of the HD and LD samples were measured at different timescales and presented in Figs. 4(A) and 4(B), where curves (i) and (ii) are for HD and LD samples, respectively. The kinetics of both samples feature an increase in absorption of the probe beam and a slow recovery after tens of milliseconds. A short spike seen at the initial stage of kinetics of both samples illustrates a strong ESA of GR1 centers with a short lifetime.

Figure 5 represents the observed optical absorption and several possible relaxation channels involved in recovery of the GR1 centers based on the pump-probe kinetics of two samples. The positive spikes at the initial stage of $-\Delta k/k_0$ kinetics at 658 nm show that there is a saturation

Optical Materials EXPRESS

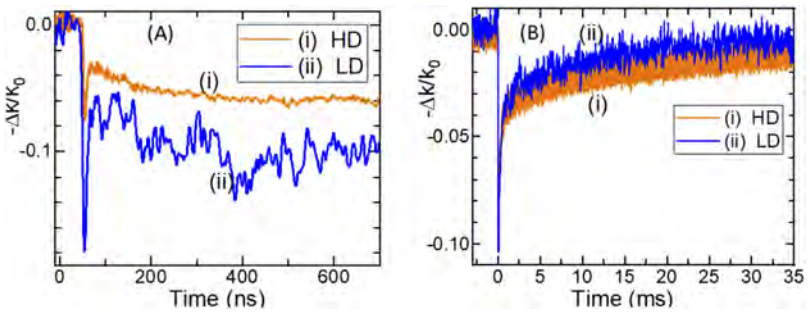

Fig. 4. The kinetics of 532 nm CW probe beam at (A) nanosecond and (B) millisecond timescales for HD (curves (i)) and LD (curves (ii)) samples.

of the absorption at 658 nm [see Fig. 3(A)], while the negative spikes of several nanoseconds at 532 nm suggests an ESA from $^1T_2$ level at this wavelength. We observed different kinetics behaviors and recovery times for 658 nm absorption in LD and HD samples. In LD samples, the absorption saturation decay with 220 µs. Considering that $^1T_2$ level lifetime was documented to be 1.1 ns at RT [18], we assume that the relaxation of the excitation occurs via metastable state. No indications of photoionization of GR1 centers at 658 nm were measured in the LD sample with pump energy fluence up to 500 mJ/cm^2. In HD sample, an additional photo-induced absorption with a long non-exponential recovery (>1 ms) was measured.

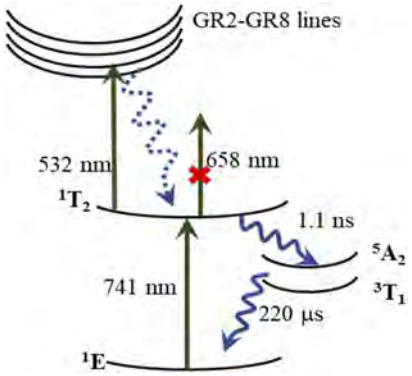

Fig. 5. Energy level diagram of GR1 centers. The straight arrows show optical absorption, and the curly arrows show the possible relaxation channels involved in the recovery of the GR1 centers based on the model proposed using 658 nm and 532 nm probe kinetics profile of LD and HD samples.

The long non-exponential recovery time (tens of milliseconds) of the induced absorption at 532 nm wavelength (Fig. 4) were measured in HD and LD samples. The most probable model for this absorption is two-photon ionization of CCs with absorption peak around 350 nm. The different decay times of the induced absorptions at 532 nm and 658 nm in HD sample and absence of induced absorption at 658 nm in LD sample suggest that these absorptions result from photoionization of different impurity centers. However, the validation of the proposed model for induced absorption bands requires a more detailed study.

3.3. Absorption saturation under 633 nm pulsed excitation

We investigated the room temperature nonlinear absorption saturation property of the GR1 centers using the setup shown in Fig. 6(A). We studied the nonlinear absorption saturation of the

Optical Materials EXPRESS

$^1E \rightarrow {}^1T_2$ transition under 633 nm pulsed excitation on LD and HD samples. The saturation of absorption of the GR1 centers in natural diamond under Q-switched Ruby laser excitation was previously reported in [22]. Also, it has been mentioned that the presence of N3 centers in the samples could manifest an additional absorption not related to the GR1 centers [22]. In our case, the pump laser was linearly polarized, and radiation attenuation was carried out by rotation of a Glan-Taylor prism. The samples were mounted on a translational stage and the incident and transmitted pump powers were measured by sliding the sample in and out of the laser beam path. A knife-edge measurement was done to estimate the beam diameter at the sample surface, which is measured to be approximately 1.2 mm at FWHM for gaussian approximation and the crystal thickness of 1 mm.

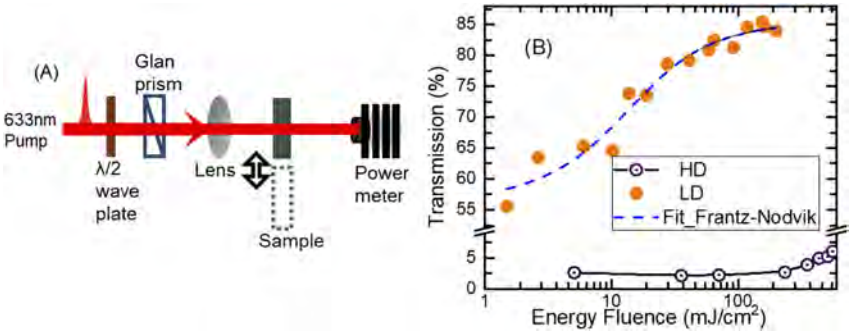

Fig. 6. (A) Experimental setup for absorption saturation measurement at 633 nm. Measured transmission of the pump signal through the samples at different input energy fluence (shown by the orange circles for LD and purple circles for HD. The measured data for LD is fitted as a slow saturable absorber predicted by Frantz-Nodvik equation for a flat top beam (plotted as a blue-dashed line).

The resulting saturation measurement of the GR1 center adjusted for the Fresnel reflection from both facets is illustrated in Fig. 6(B) with the orange and purple circles for LD and HD, respectively. For LD, as the pump energy increases, the transmission increases from its initial value of $T_0 \approx 55\%$ to the saturated level of $T_s \approx 84\%$ for a high energy fluence. It illustrates excellent bleaching of the ground level. On the other hand, HD sample revealed no noticeable saturation before the damage threshold was reached. We focus the beam to ~1 mm diameter to get a high energy fluence (~1 J/cm^2). The transmission changes from initial 2% to 8% only. It could be explained by a strong influence of photoionization process identified in HD samples in the pump-probe experiment.

In the pump-probe kinetics section, it was demonstrated that the relaxation process from the $^1T_2$ level occurs predominantly via the metastable state with a lifetime much longer than the duration of the excitation pulse. The recovery time is 220 μs, therefore the Frantz-Nodvik equation is a good approximation for this experiment. To interpret our results and extract the relevant laser parameters associated with the optical transition, we fit our experimental data for LD sample, in which saturation level was reached, to the Frantz-Nodvik solution for a slow-relaxing absorber approximated in Eq. (1) [25]:

$$T = \frac{E_s}{E_{in}} ln\left[1 + \left(e^{\frac{E_{in}}{E_s}} - 1\right) T_0\right], \tag{1}$$

where E_{in} and E_s are the input energy and saturation energy fluences, and T_0 is the initial transmission. The transmission predicted by the Frantz-Nodvik equation, shown as a dashed line in Fig. 6 (B), nicely fits our experimental data with a saturation fluence E_s=6.8 mJ/cm^2. The absorption cross-section ($\sigma_{ab} = h\upsilon/E_s$) at a pump wavelength of 633 nm was calculated to be

Optical Materials EXPRESS

4.5×10^{-17} cm^2 using the obtained value of saturation fluence. Fitting with the fast relaxation model is described in detail in our previous publication [26] which provided a very close value of cross-section (4.6×10^{-17} cm^2) at the pump wavelength.

The GR1 absorption band was obtained by subtracting the baseline [green short-dashed curve in Fig. 1(B)] from the measured absorption spectra of the LD sample. Using the absorption spectra and absorption cross-section at pump wavelength (633 nm), we calculated the absorption cross-section spectrum of the $^1E \rightarrow {}^1T_2$ transition of the GR1 center which is shown as curve (i) in Fig. 7. The cross-section curve was further utilized to calculate other spectroscopic parameters associated with the $^1E \leftrightarrow {}^1T_2$ transition relevant to laser applications. We used Eq. (2) to calculate the radiative lifetime of the excited level [27].

$$\frac{1}{\tau_{rad}} = \frac{g_l}{g_u}\frac{8\pi n^2}{c^2}\int \nu^2 \sigma_{ab}(\nu) d\nu, \tag{2}$$

where $g_l = 2$ and $g_u = 3$ are orbital degeneracies of the ground and excited states [8], respectively, c is speed of light and n is the refractive index of diamond. The radiative lifetime was calculated to be $\tau_{rad} = 8.5$ ns. The Füchtbauer–Ladenburg relation [Eq. (3)] was used to calculate the emission cross-section for transition $^1T_2 \rightarrow {}^1E$ and is depicted in Fig. 7 (curve ii). The emission cross section near the maximum of the emission band (around 780 nm) is estimated to be $\sigma_{em} \approx 9 \times 10^{-17}$ cm^2 [28,29]:

$$\sigma_{em}(\lambda) = \frac{\lambda^5}{8\pi c n^2 \tau_{rad}} \frac{I(\lambda)}{\int \lambda I(\lambda) d\lambda} \tag{3}$$

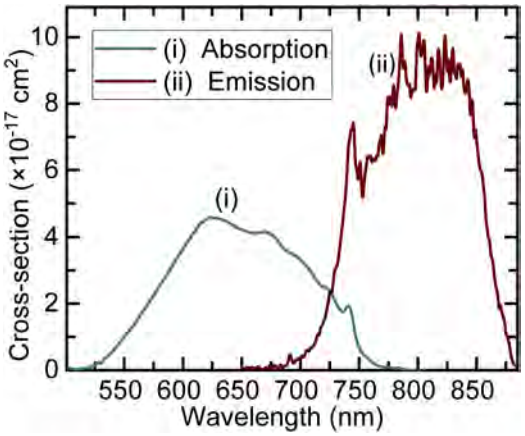

Fig. 7. Room temperature (i) absorption cross-section and (ii) emission cross-section, where the emission cross-section was calculated using reciprocity method and Füchtbauer–Ladenburg equation.

It is interesting to note that there is no "mirror symmetry" of the absorption and emission cross-sections with respect to the ZPL transition as expected for vibronic bands with linear electron-phonon coupling. As one can easily estimate from the figure, the full width at half maximum (FWHM) of the absorption and emission bands were measured to be $\Delta\nu_{abs} \approx 3600$ cm^{-1} and $\Delta\nu_{em} \approx 1800$ cm^{-1}, respectively. There are several reasons which could explain this difference. First, electron-phonon coupling could be non-linear with different effective phonon for the low and upper states. The second reason is that there is a strong energy splitting of $^1T_2$ level. In these cases, the mirror symmetry between absorption and emission bands could be broken.

Optical Materials EXPRESS

We have also estimated the quantum yield of GR1 centers $\phi = \tau_2/\tau_{rad}$ as 13% at room temperature, where lifetime of excited level (τ_2) is used to be 1.1 ns at room temperature [17]. Previously reported values for radiative lifetime and quantum yield for GR1 centers in natural diamonds were 182 ns and 0.15%, respectively, at 77 K [18]. The radiative lifetime reported in [18] was estimated from the lifetime temperature dependence. It was very sensitive to the experimental error and the fitting parameters of the considered model. Therefore, we believe that the reported lifetime in [18] are overestimated. Additionally, the radiative lifetime estimated in our work is closer to the typical radiative lifetimes of luminescent CCs in diamond, such as, for N3, H3, NV- and H4 centers 41 ns, 16 ns, 13 ns, 19 ns, respectively [30]. The authors in [30] used a very similar approach with Lorentz correction for the effective electric field to calculate the radiative lifetimes. The concentration of the GR1 centers were estimated to be 0.7×10^{17} cm^{-3} and 5.5×10^{17} cm^{-3}, respectively, for the LD and HD samples.

For laser related applications, the centers need to be stable after irradiation with a high intensity for substantial time periods. To detect any long-lived photoionization or bleaching of the centers, we measured the transmission before and immediately after (within less than a minute) illumination of the sample under 632 nm pump excitation. We irradiated the sample at sufficiently high energy fluence (>1.7 J/cm^2/pulse), which approaches the optical damage threshold. After irradiation with 10^5 pulses, our measurement showed no change in the transmission profile of both samples.

4. Conclusions

In summary, we performed a linear and non-linear optical characterization of GR1 (neutral vacancy) centers in CVD-grown bulk diamond to explore their laser feasibility. The strong saturation of absorption under 4.2 ns pulses at 633 nm wavelength was demonstrated in diamond crystals with a GR1 concentration of 0.7×10^{17} cm^{-3}. The saturation fluence E_s was estimated to be 6.8 mJ/cm^2 at 633 nm. Irradiation under 10^5 pulses with a pulse peak power of 300 MW/cm^2 revealed no long-term bleaching of the center. From the spectroscopic characterization, the maximum absorption and emission cross section were estimated to be 4.5×10^{-17} cm^2 and 9×10^{-17} cm^2 at 630 nm and 780 nm, respectively. The radiative lifetime associated with $^1T_2 \rightarrow {}^1E$ transition was calculated to be 8.5 ns. After excitation, the relaxation of the $^1T_2$ excited level occurs predominantly via the metastable state through intersystem crossing with a lifetime of 220 μs. There was no detection of ESA at 658 nm for a crystal with a GR1 concentration of 0.7×10^{17} cm^{-3}. This result indicates that these centers could be used as gain media or passive Q-switchers for laser cavities operating in a pulsed regime over the 550 - 750 nm spectral range (such as Alexandrite laser, Titanium Sapphire, Ruby lasers). However, in the case of CW laser applications, the metastable state of GR1 centers could hamper the lasing process. Also, we note that the induced absorption after excitation with pump radiation was measured at 658 nm and 532 nm wavelengths in the crystal with a GR1 concentration of 5.5×10^{17} cm^{-3}. The slow non-exponential decay of the induced absorption could arise from the recovery after photoionization of the impurity centers. The fabrication of laser gain media based on GR1 centers in diamonds require special optimization of the center concentration and crystal parameters to minimize the induced absorption at lasing wavelengths.

Funding. National Institute of Environmental Health Sciences (P42ES027723); U.S. Department of Energy (SC0018378); Air Force Office of Scientific Research (FA9550-13-1-0234).

Acknowledgement. The authors would like to thank Element 6 for providing the diamond samples.

Disclosures. The authors declare that there are no conflicts of interest related to this article.

References

1. A. M. Zaitsev, "Optical properties of diamond: a data handbook," in *Optics and Lasers in Engineering* (Springer Verlag, 2001).

Optical Materials EXPRESS

2. A. G. Mathewson and H. P. Myers, "The optical absorption of indium," J. Phys. C: Solid State Phys. **5**(17), 2503–2510 (1972).
3. S. Eaton-Magaña, "Comparison of luminescence lifetimes from natural and laboratory irradiated diamonds," Diamond Relat. Mater. **58**, 94–102 (2015).
4. J. E. Lowther, "The form of different charge states of the vacancy in diamond," J. Phys. Chem. Solids **45**(2), 127–131 (1984).
5. F. Jelezko, C. Tietz, A. Gruber, I. Popa, A. Nizovtsev, S. Kilin, and J. Wrachtrup, "Spectroscopy of single N-V centers in diamond," Single Mol. **2**(4), 255–260, (2001).
6. S. C. Rand and L. G. DeShazer, "Visible color-center laser in diamond," Opt. Lett. **10**(10), 481 (1985).
7. C. A. Coulson and F. P. Larkins, "Isolated single vacancy in diamond-I. Electronic structure," J. Phys. Chem. Solids **32**(9), 2245–2257 (1971).
8. J. E. Lowther, "Jahn-Teller coupling at ND1 and GR1 centres in diamond," J. Phys. C: Solid State Phys. **11**(9), L373–L375 (1978).
9. J. C. A. Prentice, B. Monserrat, and R. J. Needs, "First-principles study of the dynamic Jahn-Teller distortion of the neutral vacancy in diamond," Phys. Rev. B **95**(1), 014108 (2017).
10. J. Walker, "Optical absorption and luminescence in diamond," Rep. Prog. Phys. **42**(10), 1605–1659 (1979).
11. A. M. Stoneham, "The low-lying levels of the GR 1 centre in diamond," Solid State Commun. **21**(4), 339–341 (1977).
12. A. T. Collins, "Fine structure in the GR1 cathodoluminescence from natural semiconducting diamond," J. Phys. C: Solid State Phys. **11**(12), 2453–2463 (1978).
13. C. D. Clark and J. Walker, "The neutral vacancy in diamond," in *Proceedings of the Royal Society of London. A. Mathematical and Physical Sciences (1973)*, 334(1597), pp. 241–257.
14. K. Iakoubovskii, G. J. Adriaenssens, and M. Nesladek, "Photochromism of vacancy-related centres in diamond," J. Phys.: Condens. Matter **12**(2), 189–199 (2000).
15. G. Davies and A. T. Collins, "Vacancy complexes in diamond," Diamond Relat. Mater. **2**(2-4), 80–86 (1993).
16. A. T. Collins, "High-resolution luminescence-excitation spectra of the GR defect in diamond," J. Phys. C: Solid State Phys. **14**(3), 289–294 (1981).
17. A. T. Collins, J. Szechi, and S. Tavender, "Resonant excitation of the GR centre in diamond," J. Phys. C: Solid State Phys. **21**(7), L161–L164 (1988).
18. G. Davies, M. F. Thomazs, M. H. Nazares, M. Martin, and D. Shaw, "Vacancy in diamond," 13, 1–6 (1987).
19. S. D. Subedi, V. V. Fedorov, J. Peppers, D. V. Martyshkin, S. B. Mirov, L. Shao, and M. Loncar, "Laser spectroscopic characterization of negatively charged nitrogen-vacancy (NV −) centers in diamond," Opt. Mater. Express **9**(5), 2076 (2019).
20. T. Nakashima and S. Yazu, "Optical properties and laser action of H3 center in synthetic diamond," in (SPIE, 1990), pp. 10–16.
21. E. Fraczek, V. G. Savitski, M. Dale, B. G. Breeze, P. Diggle, M. Markham, A. Bennett, H. Dhillon, M. E. Newton, and A. J. Kemp, "Laser spectroscopy of NV- and NV0 colour centres in synthetic diamond," Opt. Mater. Express **7**(7), 2571 (2017).
22. V. P. Mironov, E. F. Martinovich, and V. A. Grigorov, "Laser materials based on diamond with GR1 centers," Diamond Relat. Mater. **3**(4-6), 936–938 (1994).
23. E. Fritsch and K. V. G. Scarratt, "Optical properties of some natural diamonds with high hydrogen content," in *Diamond Optics II* (SPIE, 1990), 1146, p. 201.
24. H. B. Dyer and L. D. U. Preez, "Irradiation damage in type I diamond," J. Chem. Phys. **42**(6), 1898–1906 (1965).
25. L. M. Frantz and J. S. Nodvik, "Theory of pulse propagation in a laser amplifier," J. Appl. Phys. **34**(8), 2346–2349 (1963).
26. S. D. Subedi, V. V. Fedorov, S. Mirov, and M. Markham, "Laser spectroscopic and saturation properties of GR1 centers in synthetic diamond," Proc. SPIE **11259**, 79 (2020).
27. O. Svelto, *Principles of Lasers*, 5th ed. (Springer, 2010).
28. C. C. Davis, *Lasers and Electro-Optics*, 2nd Edition (Cambridge University Press, 2013).
29. S. A. Payne, L. L. Chase, L. K. Smith, W. L. Kway, and W. F. Wyers, "Infrared cross-section measurements for crystals doped with Er^{3+}, Tm^{3+}, and Ho^{3+}," IEEE J. Quantum Electron. **28**(11), 2619–2630 (1992).
30. G. Liaugaudas, A. T. Collins, K. Suhling, G. Davies, and R. Heintzmann, "Luminescence-lifetime mapping in diamond," J. Phys.: Condens. Matter **21**(36), 364210 (2009).